ESRF	**Experiment title: (Long term report)** X-ray diffractive optical elements and differential imaging techniques for the EU RTD project TwinMic	**Experiment number**: MI-642
Beamline: ID21	**Date of experiments**: 23/7-1/8/2003 2/2-6/2/2004 4/5-11/5/2004	**Date of report**: 8-Sep-04
Shifts: 23/ 9/ 20	**Local contact(s)**: Dr. Olivier Dhez	*Received at ESRF:*

Names and affiliations of applicants (* indicates experimentalists):

Dr. Timm Weitkamp, LMN at SLS/PSI, Villigen, Switzerland*

Dr. Matteo Altissimo, TASC-INFM, Trieste, Italy*

Dr. Stefano Cabrini, TASC-INFM, Trieste, Italy*

Dr. Burkhard Kaulich, ELETTRA, Trieste, Italy*

Dr. Dan Cojoc, TASC-INFM, Trieste, Italy*

Dr. Enzo Di Fabrizio, TASC-INFM, Trieste, Italy*

Report:

1. Contributions of SLS/ PSI – Laboratory for Micro- and Nanostructuring, Villigen, CH:

The Laboratory for Micro- and Nanotechnology (LMN) at the Paul Scherrer Institut is making and testing zone plates for the scanning part of TwinMic. As a suitable zone plate material for this purpose in the energy range covered by the new instrument, tantalum had been identified already in the design phase. Ta shows reasonable diffraction efficiency at technically feasible structure values of structure thickness (Figure 1).

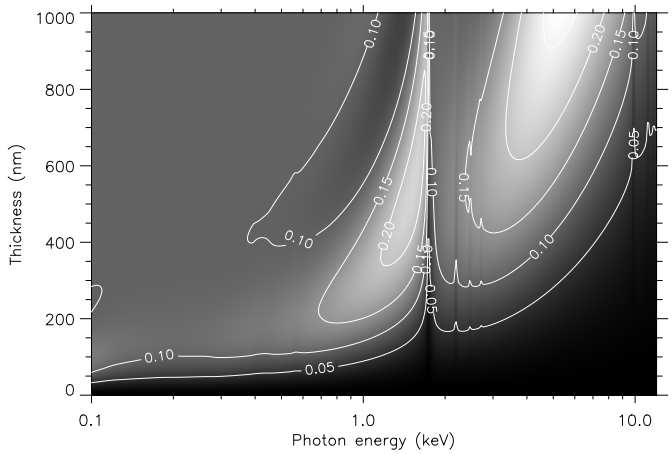

Fig. 1: *First-order diffraction efficiency for a perfect zone-plate structure as a function of photon energy and structure thickness. From [1].*

However, structuring processes for Ta depend critically on residual stress in the material and thus on deposition parameters. A magnetron sputtering machine that allows fine yet reproducible tuning of the deposition conditions is on loan from ESRF at the LMN and is used for Ta deposition. The zone plate pattern is generated with electron-beam lithography using LMN's e-beam machine (Leica LION LV1). The structure transfer from electron resist into the tantalum layer requires several steps, sketched in Figure 2.

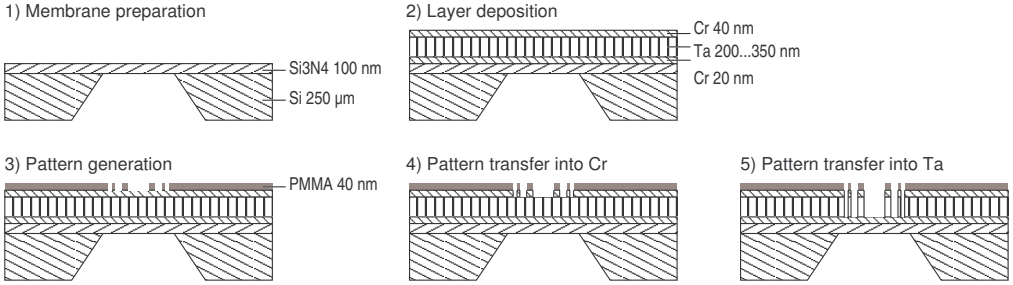

Fig. 2: *Process steps for production of tantalum zone plates. On a silicon-nitride membrane, Ta is deposited as well as thin Cr films acting as etch-mask and etch-stop layers. After pattern generation with electron-beam lithography, the structure is transferred into the tantalum in two consecutive dry-etching steps. From [2].*

As a support structure, silicon-nitride membranes with thickness between 100 and 250 nm are used. A central stop, blocking the zeroth diffraction order, can be deposited on the back side of the nitride membrane by alignment of the zone plate over a pinhole of suitable diameter and subsequent evaporation of gold through the pinhole onto the membrane (Figure 3).

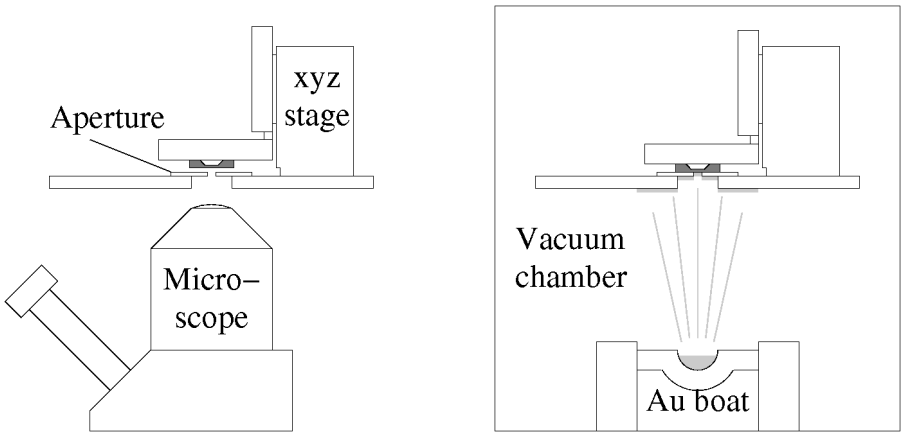

Fig. 3: *Procedure for the deposition of a central stop. Left: Alignment of the zone plate over a pinhole aperture over a microscope. Evaporation of gold through the aligned aperture.*

Using this fabrication process, zone plates with diameters between 250 and 500 µm and tantalum-layer thicknesses of 200, 250, and 300 nm were produced. The outermost zone width is 80 nm for all devices made. Figure 4 shows scanning electron micrographs of two samples. Efficiency and resolution measurements for these devices were carried out at ID 21 in several beamtimes, most at photon energy of 2.5 keV, where the focal lengths of the lenses range between 40 and 80 mm, depending on their diameter. Efficiency measurements of the 200-nm-thick zone plates yielded values close to the optimum value for the test photon energy, i.e., an efficiency of 6 %. The efficiencies measured for the thicker lenses was, however, considerably below the theoretical values, probably due to etching problems during the structure transfer into tantalum. A test of spatial resolution was carried out with a zone plate of 250 µm diameter and 200 nmthickness. A gold test object with varying line width was scanned through the focal spot of the zone plate and the transmitted intensity recorded at every scan point. The smallest lines of the test object, with a

width of 100 nm, were still resolved with 4 % contrast, or one-sixth of the DC contrast of the object (Figure 5).

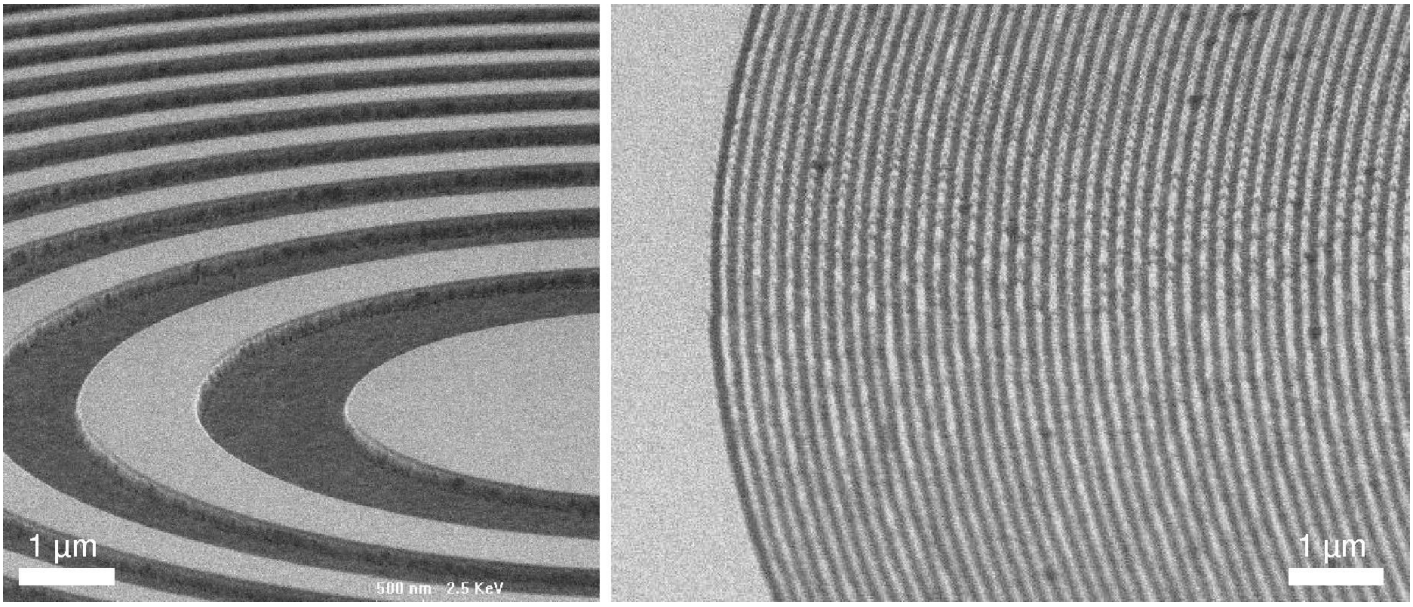

Fig. 4: *Electron micrographs of two of the tantalum zone plates produced. Left: central part, right: outermost zones. From [2].*

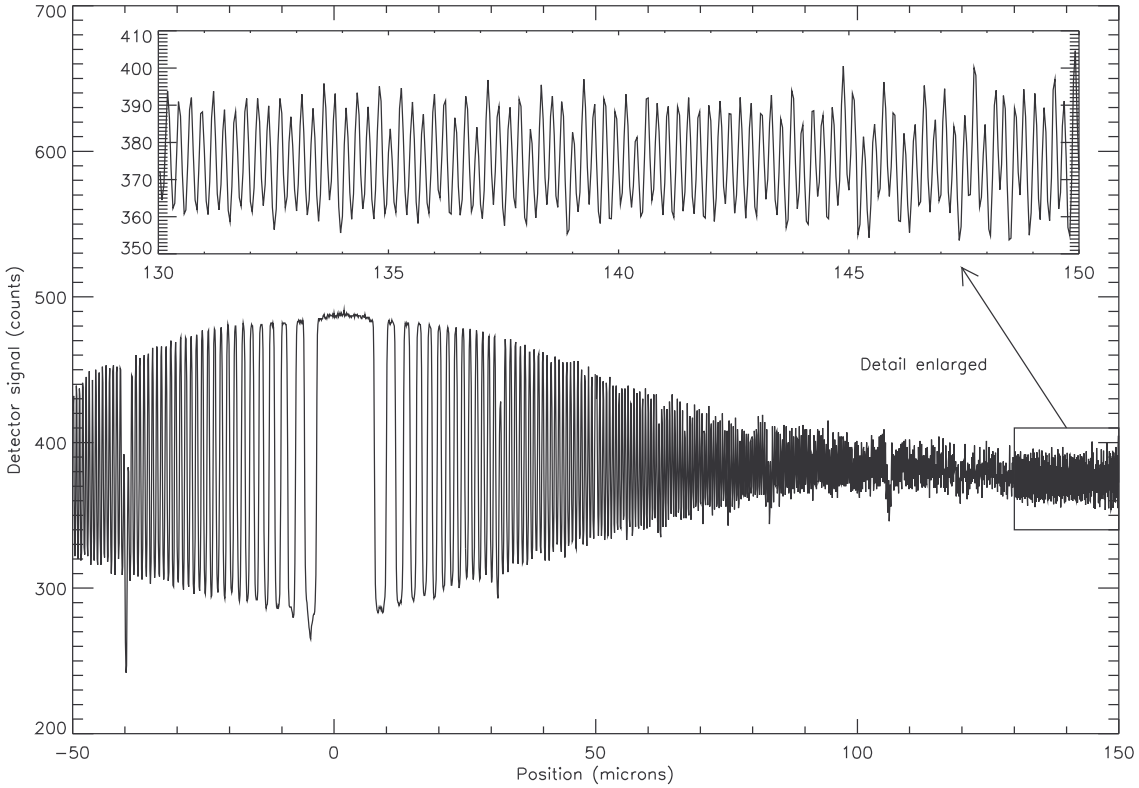

Fig. 5: *Result of a resolution test with a 200-nm-thick, 250-µm-diameter zon e plate with 80-nm-wide outermost zones. A gold test structure with varying line width was scanned through the focal spot. From [1].*

In addition to process development and zone-plate fabrication, some new zone-plate pattern designs were developed. In particular, a pattern for a twin-spot zone plate was developed that is compatible with the LMN e-beam machine and its continuous-path-control mode of operation.
Zone plates that create two laterally separated focal spots are useful in differential interference contrast methods recently developed for full-field and scanning X-ray microscopy. In order to

produce two spots, the diffraction pattern of a normal zone plate is superimposed with a linear phase grating. While the period of the grating determines the spot separation, the phase of the grating lines with respect to the center of the concentric ring pattern of the zone plate controls the relative phase of the light field in the two spots. Figure 6 shows the principle. Higher-order spots in the lateral intensity distribution can be suppressed by introducing blank lines in the linear-grating pattern. Zone plates using this principle were fabricated and one of them tested at ID 21. Figure 7 shows measured spot profiles of a twin-spot zone plate with this design.

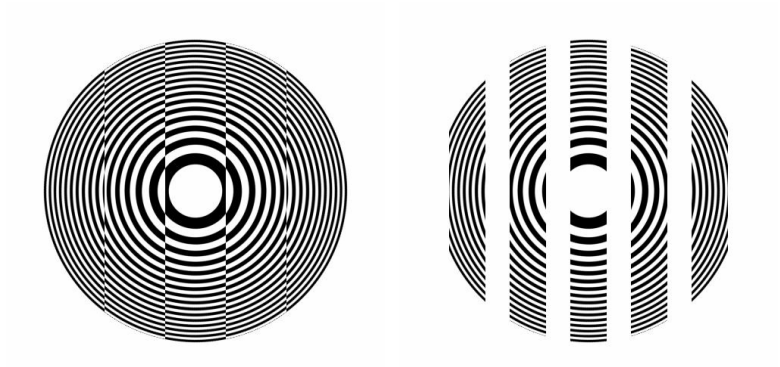

Fig. 6: *Design of a zone plate with two laterally separated spots. Left: superposition of a circular zone plate pattern with a linear phase grating. Right: Introduction of blank stripes to suppress higher-order spots. From [2].*

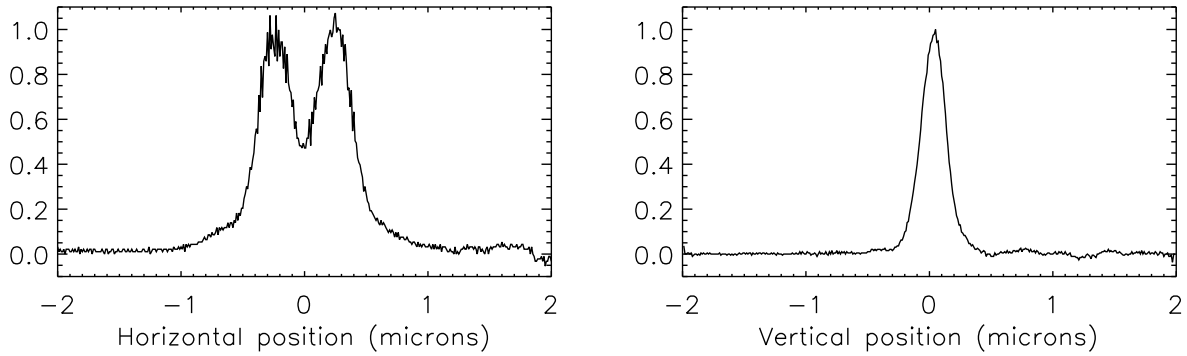

Fig. 7: *Horizontal (left) and vertical (right) spot profile of a tantalum twin-spot zone plate, measured at ID 21 with 2.5-keV X rays. From [2].*

References:

[1] T. Weitkamp, B. Kaulich, O. Dhez, and C. David, First tantalum zone plates for the TWINMIC X-ray microscope, Microelectron. Eng. 73-74 (2004) 651-655.

[2] T. Weitkamp, O. Dhez, B. Kaulich, and C. David, *Tantalum zone plates for scanning X-ray microscopy between 0.5 and 2.5 keV*, in Design and Microfabrication of Novel X-Ray Optics II, edited by A. A. Snigirev and D. C. Mancini, Vol. 5539 of Proceedings SPIE, Bellingham, WA, SPIE, paper no. 5539-20, in the press.

2. Contributions of TASC/ INFM, Trieste, I:

In the last decade there was an increased interest for Extreme UltraViolet (EUV) and X-Ray Microscopy, due to the characteristics of the beam delivered by third generation synchrotron radiation sources [1]: high brightness, low beam divergence and almost monochromatic spectrum, tunable over a range of several keV in photon energy. Synchrotrons of the latest generation and free electron lasers, in the near future, are devices that produce x-rays with these characteristics.

With the availability of a source of electromagnetic radiation bright enough (i.e. point-like and monochromatic) new possibilities open up for the designer of optical instrumentation. This is what is happening with x-ray microscopes of the latest generation [2,3]. Nevertheless, up until now the focusing element in a x-ray microscope has not evolved far beyond the conventional zone plate (ZP), invented more than hundred years ago. ZPs are since twenty years a common choice as focusing elements in x-ray microscopes, due to technological improvements that took place in this framework of time [4,5].
In this paper we extend the ZP concept to a more general category of Diffractive Optical Elements (DOEs) that can perform specific optical functions. In particular, the phase and intensity distribution of the incoming wave can be shaped with almost complete freedom. We describe the design, the fabrication and tests of two types of DOEs, used in transmission and scanning x-ray microscopes. One is a novel holographic condenser (HoCo) that will produce a so called top-hat intensity distribution, and the second is a phase DOE that is able to focus the x-ray beam into two spots in the plane perpendicular to the optical axis, with a relative controlled phase shift between the spots.
The reason of introducing a new kind of condenser in a transmission x-ray microscope lies in the high degree of spatial coherence of the source. A ZP condenser produces a spot in the object plane much smaller than the desired object field. As an example, if we assume an x-ray source size of 200 μm (typical of an undulator in an electron storage ring) and a distance of 50 m from the experimental station, a condenser ZP with focal length f=1 m will form a spot of approximately 4 μm in the object plane of the microscope, where the required value would be 20-50 μm. By using a longer focal length ZP, a bigger focal spot can be obtained, with the drawback of very small Numerical Aperture (NA), which has to be matched by the one of the objective ZP.
Therefore in the case of microscopy a homogenously illuminated field is more desirable with respect to a small spot. Our idea is now to make a hologram of a scattering screen that will be reconstructed with the size of the required object field bye the incoming, almost parallel, light. This task can be accomplished by defining the desired light distribution in the object plane in such a way that the amplitude of the light is constant in the object field, zero elsewhere (that is, a top-hat intensity distribution), and the phase varies randomly on a lateral scale length given by the spatial resolution of the microscope objective. The phase needs to be randomly distributed in order to provide a low degree of spatial coherence in the illumination path of the microscope, so as to exploit better the spatial resolution, and to suppress side lobes in the diffraction pattern of object edges.
A phase DOE opens up the possibility to perform differential phase contrast and Differential Interference Contrast (DIC) microscopy also with x-rays, similar to the Normarski configuration in visible light [6-9]. The second contrast method is widely used to investigate transparent samples. DIC converts gradients in the object optical path length into amplitude differences that can be visualized as improved contrast in the resulting image. The phase object is sampled by two mutually coherent waves that have a lateral displacement □x, called the shear, and a phase displacement, □□called the bias. If the shear is of the order of the object details, it is imaged into an intensity distribution that is a function of the spatial gradient of the object phase distribution [10]. It is useful also to control the bias, in order to exploit the phase function of the imaged object. A practical consequence is the contrast enhancement for biological samples, when the thickness is irregular. We would like to underline that, in our knowledge, is the first time that a control in the bias retardation is reported.
In section 2 we will describe the design the simulations and the fabrication of our novel DOEs. In Section 3 we will show the results of our experiments at ESRF ID21 beamline [11], and in Section 4 we will discuss the results obtained.

Design and fabrication

Phase DOEs are known as optical elements that convert a specified illumination wave into a desired distribution of its phase, amplitude or polarization, by modulating only the phase of the incoming electromagnetic field. Several different efficient iterative techniques are available for the

design phase DOEs with surface relief modulation for visible light [12], and in a recent papers [13] we have shown that these approaches can be extended to design phase DOEs also for x-rays.

1 Design

The Holographic Condenser and the objective DOEs have been designed following two different strategies, which are going to be explained separately.
In the case of the condenser, we used our own code based on scalar diffraction theory and thin element approximation. The software is able to calculate the surface relief modulation of an optical element, by specifying the desired electromagnetic field configuration in the object plane, the illumination conditions, the size of the DOE and the minimum pixel size[14].
In the specific case of HoCo the working photon energy is set at 4 keV, with an illuminated square field in the object plane of 25.6 μm in lateral dimension, and minimum pixel size of 200 nm. The focal length of the condenser was chosen to be 267 mm. Figure 1 shows the bitmap 2048x2048 pixels image of the condenser produced by our code.

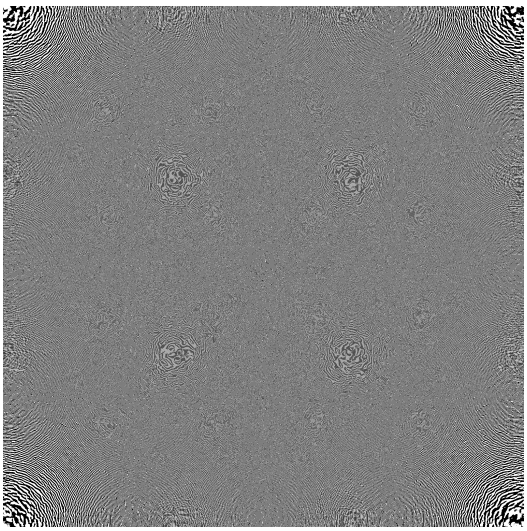

Fig. 1: *General view of the software-generated top-hat condenser. The software produces a bitmap 2048x2048 pixels, 200 nm pixel size. This leads to a lateral dimension of about 410 μm. The condenser is designed to give a top-hat intensity distribution on a 25.6 x25.6 μm square, with a focal length of 267 mm at 4 keV incident photon energy.*

We performed the design of the objective DOEs following a different strategy. A phase DOE that accomplishes beam shearing in DIC microscopy can be seen as an element that generates two spots with a specified phase difference between them. This is a special case of a more general situation, in which a DOE, illuminated by a set of point sources, generates a set of spots in a determined confiration. This DOE can be calculated by a direct approach, assuming that both the light sources illuminating the DOE and the so-generated pattern can be described by point sources that emit spherical waves. In this approach, an estimate for the phase function is given by the superposition of spherical wavefronts at the DOE plane. By assuming that the DOE is a thin element described by its transmittance function: $t(x,y)=\exp[i\Phi(x,y)]$, with the phase function $\Phi(x,y)$: R^2 [0, 2π). If $W_{in}(x,y,0)$ represents the complex amplitude of the incident wave, under the assumption of the thin element approximation, the complex amplitude of the output wave after the DOE will be:

$$W_{out}(x,y,0) = t(x,y)W_{in}(x,y,0) \quad (1)$$

Where z=0 denotes the DOE's plane. For a given input-output of pair waves, satisftying the condition :

$$|W_{in}(x,y)| = |W_{out}(x,y)| \quad (2)$$

the phase function is given by:

$$\Phi(x,y)= \{\arg[W_{out}(x,y,0)] - \arg[W_{in}(x,y,0)]\}_{2\pi} \quad (3)$$

where the subscript 2□states for modulo 2□If the source and the generated spots are described by a set of N_s and N_g points respectively, with $\{P_s(x_s,y_s,z_s),\ s=1,N_s\}$ and $\{P_g(x_g,y_g,z_g),\ g=1,N_g\}$, the expression for the input and the output waves and the point $P_e(x_e y_e,0)$ at the DOE plane will be:

$$W_{in}(x_e,y_e,0) = \sum_s a_s \cos\psi_{s,e} \frac{\exp[jkr_{s,e}]}{r_{s,e}} \quad , \quad W_{out}(x_e,y_e,0) = \sum_g a_g \cos\psi_{g,e} \frac{\exp[j(kr_{g,e}+\varphi_g)]}{r_{g,e}} \quad (4)$$

where $a_{s(g)}$ are constants representing the amplitudes of the waves emitted by the point sources, $\cos\psi_{s,e} = z_s/ r_{s,e}$ is the obliquity factor, $r_{s,e}=P_sP_e$ is the distance between the source point P_s and the element P_e of the PDE, $r_{g,e}=P_gP_e$ is the distance between the source point P_g and the element P_e of the DOE, φ_g is the initial phase of the point P_g and k is the wavelength number $k=2\pi/\lambda$. Using the equations (3) and (4) the phase function is calculated for the set of sampling points $\{P_e(x_e,y_e,z_e),\ e=1,N_e\}$ defined by a regular spaced squared grid on the DOE. The number of the sampling points N_e is limited by the scalar diffraction approximation and the sampling theorem to: $D/2\lambda < N_e < D^2/\lambda z$, where D is the lateral size of the DOE and z represents the distance from the source plane or the plane of the generated spots to the DOE.

We decided to implement a DOE that generates two spots, 50 mm downstream the optical element at 4 KeV photon energy. The shear between the spots is 200 nm, and the bias retardation is 0 radians. In Figure 2 we show the results of these simulations, together with the optical function of the element.

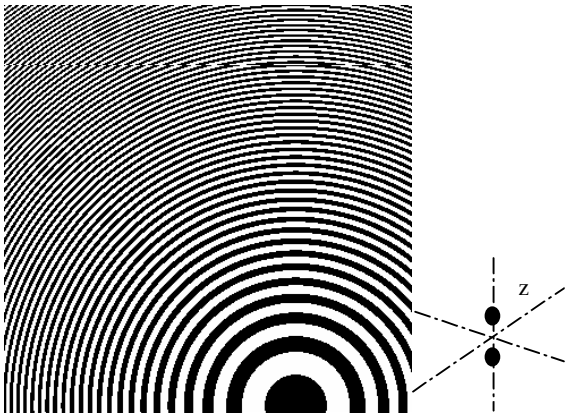

(a) (b)

Fig. 2*: (a) Details of the software-generated DIC objective. The focal length of the DOE is 50 mm at 4 keV photon energy, a shear of 200 nm, and a bias retardation of 0 radians. In this case, the bitmap is (b) image of the optical function performed by the DOE.*

2 Fabrication.

Following the approach described in the previous section we have developed our own code to calculate phase DOEs which work in the range of x-ray wavelengths. The phase function is implemented by modulating the thickness of the gold absorber grown on a silicon nitride membrane. The spatial variation of the thickness is given by:

$$d(x,y) = \Phi(x,y)\lambda/2\pi\alpha(\lambda) \quad (5)$$

where 1-α is the real, phase-shifting part of the refractive index. For all materials at X-ray wavelength 1-α is very close to unity. For instance, for the gold $\alpha(\lambda)\in[1.8\ 10^{-4}, 30\ 10^{-4}]$ for $\lambda\in[3, 16.31]$ Å and a 2π phase shift leads to a maximum surface profile: $d_{max}\in[1667, 543]$ nm. Considering δ ~ 50 nm the typical minimum feature size that can be achieved by modern microfabrication techniques, the condition for the thin element approximation is satisfied at the limit ($\delta>\delta_{min}\in[31.6, 41.81]$ nm) since the wavelengths are very short. On the other hand, $\delta >> \lambda$ and therefore the scalar diffraction theory can be also applied. In terms of the f-number f/D (where f is the focal length and D is the diameter of the DOE), the minimum f/D that can be obtained for a DOE working at X-ray wavelengths is: $f/D_{min} = 87$ for λ=3 A and $f/D_{min} = 21.2$ for λ=16.1 Å.

On the basis of the above mentioned considerations, we have fabricated two phase DOEs for a photon energy of 4 keV, by a combinated use of Electron Beam Lithography (EBL) and the X-Ray Lithography (XRL). The XRL step is needed in order to replicate the DOEs pattern on the optimized phase shifter thickness for a photon beam of 4 KeV in energy. The phase shifter chosen is gold, and the optimized thickness is about 900 nm.

The top-hat and the phase binary DOEs XRL masks, 0.4x0.4 mm^2 and 0.1x0.1 mm^2 size respectively, with the minimum structure size of 200 nm for the condenser and 100 nm for the DIC objective, were fabricated with an EBL system using a Raith ELPHY pattern generator. The bitmap file generated by our codes were transferred to the Raith pattern generator. A 300 nm PMMA 950-K layer was spun on a 2 μm silicon nitride membrane covered by a thin chromium gold base plate. After the exposition and development of the resist the patterned gold absorber was grown by an electrolytic process. In this way we obtained the x-ray masks, that were subsequently replicated using the XRL experimental station hosted at LILIT beamline [15], Elettra Synchrotron in Trieste (Italy). In this latter step, a 1 □m PMMA 950-K layer was spun on a 2 μm silicon nitride membrane covered by a thin chromium gold base plate and then exposed to the photon beam. After the development of the resist, the required thickness of gold was grown by an electrolytic process. In Figure 3 we show the obtained top-hat condenser and the DIC objective.

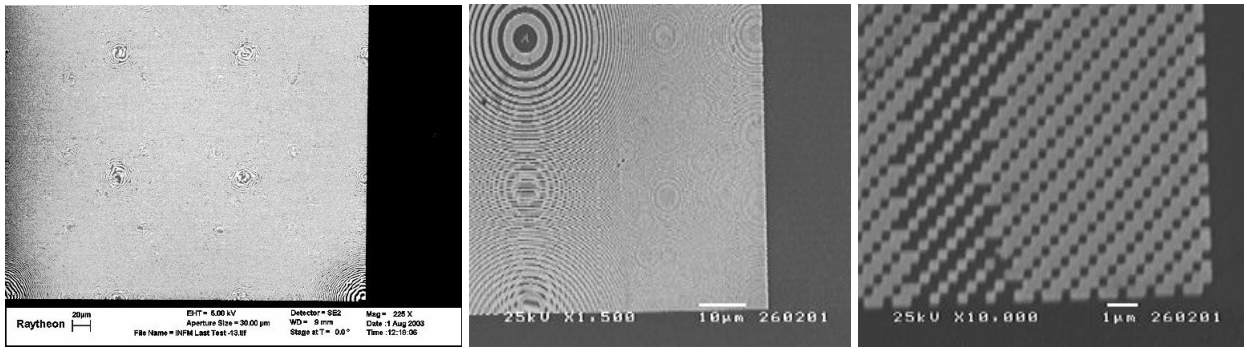

(a) (b) (c)

Fig. 3: *Scanning Electron Microscope (SEM) images of the XRL fabricated optical elements. (a) total view of the holographic condenser. (b,c) SEM pictures showing an overview (b) of the DOE that generates two spots and details of the outermost area (c) with 100 nm resolution.*

Experimental tests

The experiments were performed at ID21 laboratory on the full-field imaging and the scanning x-ray microscope branch lines of the ESRF (European Synchrotron Radiation Facility in Grenoble). The full field branch line is operated at 4 keV photon energy. The monochromaticity of $\Delta E/E=10^{-4}$ is provided by a Si<111> double crystal monochromator. The optical scheme of the full-field imaging microscope, depicted in Fig. 4.a, is similar to a conventional transmission microscope with

critical illumination. The top-hat condenser focuses the light onto the sample and then a magnified image (150x) is obtained through the phase DOE objective onto a spatially resolving detector.

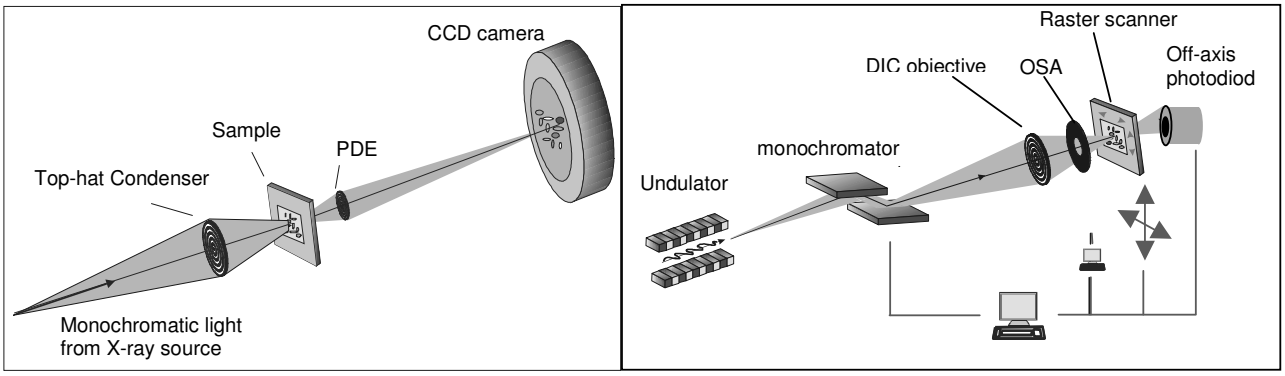

(a) (b)

Fig. 4: *Optical layout of the x-ray microscopy station at ID21, European Synchrotron Radiation Facility (ESRF), Grenoble (France). (a) shows the layout of the full field and (b) the one of the scanning x-ray microscopes.*

Figure 4.b shows the optical layout of the scanning x-ray microscope, where the DIC objective tightly focuses a monochromatic x-ray beam onto the sample, which is raster scanned. The detector collects the intensities for each pixel in the scansion, and the whole topography is reconstructed via software. Furthermore, at ID21 an X-Ray Fluorescence detector can be mounted near the sample. In this way, by varying the incoming photon energy according to the absorption edges of desired elements, it is possible to map also the elemental presence in the sample.
The full field setup was used at 4 KeV photon energy, with our top-hat condenser and the DIC objective. The typical exposure time was about 30 seconds. We took images of some test structures made on PMMA resist by EBL. The finest structures are separated by a gap of 120 nm. Figure 5 shows the results of our exposures. The finest structures are quite clearly resolved, but we would like to point out that this was a test mainly for the top-hat condenser.

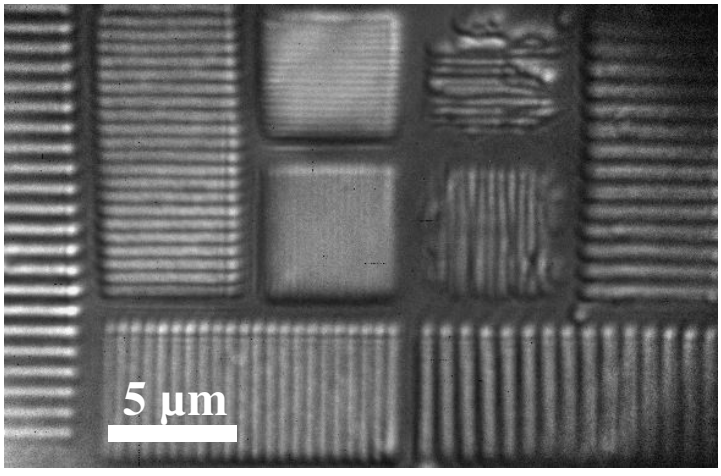

Fig. 5: *A full-field x-ray microscope image of a resist test pattern. The images have been collected at 4 keV photon energy, where the resist has a transmission of about 99.99%. The image was recorded using the top-hat condenser and a DIC objective, and an exposure time of 30 seconds.. The finest structure on the image are separated by 120 nm, quite well resolved by our optical setup.*

References

[1] D. Attwood, *"Soft x-rays and extreme ultraviolet radiation; principles and applications",* Cambridge University Press, (1999).

[2] G. Schneider, "*Cryo X-ray microscopy with high spatial resolution in amplitude and phase contrast*," Ultramicroscopy **75**, 85-104, (1998).

[3] G. Schmahl, D. Rudolph, G. Schneider, P. Guttmann, B. Niemann, "*Phase-contrast X-ray microscopy studies*," Optik **97**, 181-182, (1994).

[4] A. G. Michette, "*Optical Systems for Soft X-rays*", Plenum Press, New York, (1986)

[5] E. Di Fabrizio, F. Romanato, M. Gentili, S. Cabrini, B. Kaulich, J. Susini, R. Barrertt, "*High efficiency multilevel zone plates for keV X-rays*",Nature **40**, 895-898, (1999).

[6] F. Zernike, " Phase contrast, a new method for the microscopic observation of transparent 8. objects," Physica **9**, 686-698 (1942).

[7] G. Normarski, and A.R. Weill, "*Application à la métallographie des methods interférentielles à deux ondes polarisées*", Rev. Metall. **2**, 121-128, (1955).

[8] G. Schmahl, D. Rudolph, G. Schneider, P. Guttmann, B. Niemann, "*Phase-contrast X-ray microscopy studies*", Optik **97**, 181-182, (1994)

[9] B. Kaulich, T. Wilhein, E. Di Fabrizio, F. Romanato, M. Altissimo, S. Cabrini, B. Fayard, and J. Susini, "*Differential interference contrast X-ray microscopy with twin zone plates*", J. Opt. Soc. Am A **19**, 797-806 (2002)

[10] E. Di Fabrizio, D. Cojoc, S. Cabrini, B. Kaulich,J. Susini, P. Facci, T. Wilhein, *"Diffractive optical elements for differential interference contrast x-ray microscopy"*, Optics Express, Vol 11, 2278-2288, 2003.

[11] J. Susini, R. Barret, B. Kaulich, S. Oestreich, and M. Salomé, "*The X-ray microscopy facility at the ESRF: A status report* ", AIP Conf. Proc. **507**, 19-26 (2000).

[12] V. Soifer, V. Kotlyar & L. Doskolovich, "*Iterative methods for diffractive optical elements computation*", Taylor-Francis Ltd, (1997).

[13] E. Di Fabrizio, D. Cojoc, S. Cabrini, B. Kaulich, T. Wilhein, J. Susini, "*Novel diffractive optics for x-ray beam shaping*", SPIE Proc. **4783**, 105-114 (2002).

[14] E. Di Fabrizio E, Cabrini S, D. Cojoc, Romanato F, Businaro L, Altissimo M, Kaulich B, Wilhein T, Susini J, De Vittorio M, Vitale E, Gigli G, Cingolani R, "*Shaping X-rays by diffractive coded nano-optics*", MicroElectronic Engineering, 67-68: 87-95, (2003).

[15] Filippo Romanato, Enzo Di Fabrizio, Lisa Vaccari, M. Altissimo, D. Cojoc, L. Businaro, Stefano Cabrini,*"Lilit Beamline for Soft and Deep X-Ray Lithography at Elettra",* MicroElectronic Engineering (57-58) 2001.